Conclusion

Calculations based upon simple strip theory show that a nonlinear aerodynamic method predicts a minimum divergence speed in the transonic range which is associated with the rearward shift of aerodynamic center. In addition, airfoil shape has a significant influence upon divergence as shown by a 17% difference in minimum divergence dynamic pressure between a supercritical wing and a conventional wing. Although the relative sensitivity of various airfoil shapes to divergence may be assessed by the strip theory approach used here, sophisticated, three-dimensional transonic aerodynamic methods should be employed to predict wing divergence characteristics accurately.

References

[1] Bisplinghoff, R.L., Ashley, H., and Halfman, R.L., *Aeroelasticity,* Addison-Wesley Publishing Co., Reading, Mass., 1955, pp. 479-481.

[2] Bauer, F., Garabedian, P., Korn, D., and Jameson, A., "Supercritical Wing Sections II," *Lecture Notes in Economics and Mathematical Systems,* Vol. 108, Springer-Verlag, New York, 1975.

C.80-133

Analysis of High Velocity Impact on Hybrid Composite Fan Blades

80003
80006

C. C. Chamis* and J. H. Sinclair†
NASA Lewis Research Center, Cleveland, Ohio

Introduction

APPLICATION of advanced fiber composites to turbine engine fan blades offers several potential advantages. The most significant of these are: 1) elimination of the midspan shroud which results in improved engine efficiency, 2) lighter engine and aircraft weights which result in reduced fuel consumption, and 3) higher possible tip speeds which can reduce the number of fan or compressor stages and result in fewer parts and lower initial and operating costs.

One major problem with the application of advanced fiber composites to fan blades has been their low resistance to impact in general, and to bird ingestion and other foreign object damage (FOD) in particular. A major difficulty in predicting impact resistance of composite fan blades has been the limitations of available analysis methods for coping with the complex problem of predicting the local and global dynamic response when subjected to high velocity impact. This paper describes recent developments in the analysis of high velocity impact of composite blades using a computerized capability which is under development at the NASA Lewis Research Center.

Briefly, at the present stage of development, the method consists of coupling a composite mechanics computer code with the direct-time integration feature of NASTRAN. All aspects of composite mechanics from micromechanics to laminate analysis and combined stress failure are handled via the composite mechanics computer code. The structural dynamics aspects of the high velocity impact are handled via NASTRAN. The discussion of the application of the computerized method in this paper is limited to the linear dynamic response of an interply hybrid composite fan blade subjected to a high velocity impact of a 2 lb bird.

Presented as Paper 79-0783 at the AIAA 20th Structures, Structural Dynamics, & Materials Conference, St. Louis, Mo., April 4-6, 1979. This paper is declared a work of the U.S. Government and therefore is in the public domain.

Index categories: Structural Composite Materials; Structural Dynamics.

*Aerospace and Composite Structures Engineer. Member AIAA.

†Aerospace Materials Engineer.

Blade Geometry, Hybrid Composite, and Finite Element Model

A photograph of the blade investigated is shown in Fig. 1. The blade was designed and made by the General Electric Co.[1] The nominal dimensions of the blade are 21 in. long, and 12 in. wide at the tip. The thickness varied along the blade centerline from about 0.90 in. at the root to 0.30 in. at the tip. The nominal leading and trailing edge thicknesses were 0.13 in. The angle of twist was approximately 33 deg. The nominal tip radius from the center of the shaft was about 35 in.

The interply hybrid composite blade consisted of boron/epoxy outer plies at ±45 deg (measured from the radial line), S-glass/epoxy plies at 0 and ±45 deg near the root, S-glass cloth filler plies at the root, and Kevlar 49/epoxy plies at 0, ±45, and 90 deg interspersed through the thickness of the blade. The blade also had metallic leading edge protection. The total number of different materials in the hybrid composite blade was five. The nominal ply thickness was 0.010 in. The fiber volume ratio was about 0.60. The several 0 and ±45 deg S-glass/epoxy plies near the root were added to increase bending strength of the blade for improved impact resistance.

The blade was modeled using 127 nodes (grid points) and 210 anisotropic-material, triangular plate elements (CTR1A2 in the NASTRAN[2] element library). Each element had different material properties (Fig. 2).

Analysis, Results, and Discussion

The high velocity impact analysis of the hybrid composite blade was performed using the computerized capability depicted schematically in Fig. 3. This computerized capability

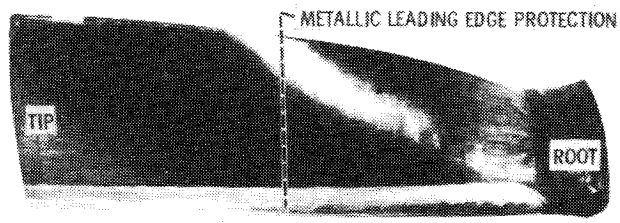

Fig. 1 Hybrid composite fan blade nominal dimensions (21 in. long, 12 in. wide at tip).

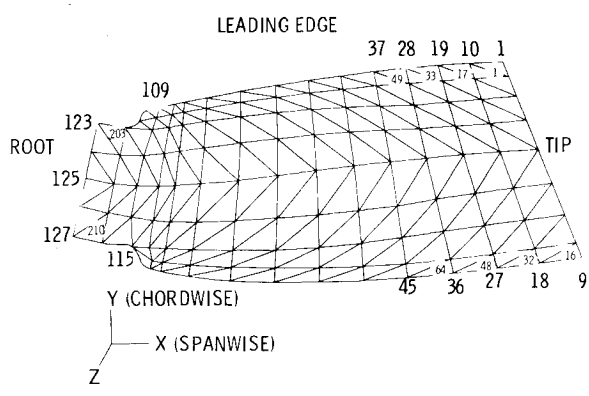

Fig. 2 Hybrid composite fan blade finite element representation schematic (127 nodes, 210 elements, 210 material properties).

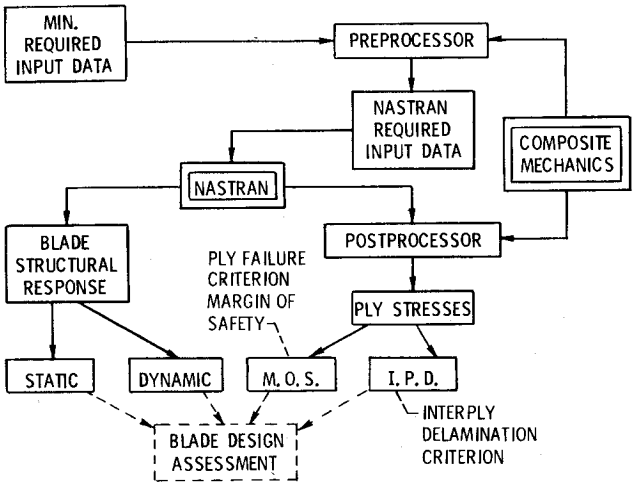

Fig. 3 Computerized capability for composite blade high velocity impact analysis (NASTRAN coupled with composite mechanics).

consists of two major modules: NASTRAN[2] and composite mechanics[3] which communicate with each other via a pre- and a postprocessor. Parts of this computerized capability have been used extensively for the analysis of composite blades.[4-6]

Input Data

The input data for the blade was supplied for four span sections: bottom of root, beginning of airfoil, midspan of airfoil, and tip. The remaining blade geometry, grid (nodal) point coordinates of grid point, thickness, and element connection cards were generated by the preprocessor. The number of plies at each grid point, ply stacking sequence, and ply type were also generated by the preprocessor. The ply properties were generated by the composite micromechanics available in the composite mechanics module which accesses a computer resident composite material properties data bank via the preprocessor. The ply properties, stacking sequence, composite system, and number of plies (including the metalic leading edge) were used in the laminate analysis (available in the composite mechanics module) to generate the laminate properties at each grid point. The laminate properties at each grid point were then used in the preprocessor to generate the properties (MAT2 and PTRIA2) for each element (210 elements, see Fig. 2). The information in each MAT2 card consisted of four stress-strain coefficients, density, and three thermal expansion coefficients.

The boundary conditions simulating blade attachment consisted of fixing the x and z displacement of grid points 123-127 (Fig. 2), the y displacement in grid point 125, and the three rotations of grid points 123-127. In addition, the global z rotation was constrained in grid points 109-127 (Fig. 2). These boundary conditions were entered manually in the NASTRAN bulk data via single point constraint (SPC) cards. The rotation speed, the forcing function simulating the bird impact, and the impact region (to be described later) were entered manually using the appropriate NASTRAN bulk data cards.

Vibration Frequencies and Steady State Loads

In order to confirm that the interply hybrid composite blade was properly modeled, the first five cantilever vibration frequencies were computed and compared with available measured data. The results are summarized in Table 1. As can be seen the predicted results are within 7% of the measured data. This agreement is considered to be excellent in view of the fact that the hybrid composite blade consists of five different materials varying in amount and direction at each grid point.

Table 1 Vibration frequencies (cps) of hybrid composite fan blade

Mode	Measured[a]	Predicted	Predicted / Measured
1	62	64	1.03
2	190	186	0.98
3	288	303	1.05
4	425	454	1.07
5	667	653	0.98

[a] Ref. 1.

The steady state loads consist of the aerodynamic pressures and temperatures and centrifugal loads due to the rotation of the blade in general. Previous studies[5] have shown, however, that the aerodynamic loads (pressures and temperatures) produce negligible stresses (less than 5%) in the blade compared to the stresses produced by the centrifugal loads. The stresses due to centrifugal loads were determined using the shaft rotational speed of 3157 rpm. The calculated composite average stresses in the radial direction were less than 10 ksi in the airfoil. The stress was 12 ksi at the transition region from the airfoil to the root near the trailing edge (Fig. 2), and 10 ksi at the point of blade maximum thickness near the blade midchord. These calculated stresses were within about 11% of those determined from strain gage data (respectively, 13.5 and 9 ksi).[1] An agreement within 11% between calculated and predicted composite stress is considered very good for the reasons mentioned previously.

The vibration frequencies and centrifugal stress comparisons provide confidence that hybrid composite blades with complex geometries and made from several materials can be modeled adequately using the computerized capability depicted schematically in Fig. 3. It is reasonable to conclude, then, that this computerized capability will describe the response of hybrid composite blades, and of composite blades in general, with reasonable accuracy when these blades are subjected to high velocity impact prior to the onset of local damage anywhere in the blade.

High Velocity Impact

The analysis for the high velocity impact was performed using the direct time integration capability of NASTRAN (Rigid FORMAT 9). The global mass and stiffness matrices were generated by NASTRAN using the information from the input data described previously. The damping matrices were generated by NASTRAN using a damping factor of 0.005 and the first vibration frequency (with geometric stiffening) of 74 cycles per second (cps).

The impact force vector used in the analysis was provided by the contractor[1] and is shown in Fig. 4. It peaks at about 15,000 lb and acts on the blade (contact time) for approximately 0.5 ms. The impact conditions represented by this force vector are as follows: 1) rotor speed, 3157 rpm; 2) incidence angle, 33 deg; 3) impact location 80% of span, approximately 32 in. radius; 4) bird relative velocity, 927 ft/s; 5) bird weight, 2 lb; and 6) bird slice, 8 oz. The impact force vector (Fig. 4) was assumed to act on the blade along the grid point line containing nodes 19-27 (Fig. 2) for analysis purposes.

Typical transient results obtained from this analysis for blade tip displacement and composite stresses at the impact point are described below.

The z component of the leading edge tip displacement vs time is shown in Fig. 5. The contact time and estimated maximum tip displacements from high speed movies are also shown in this figure. The interesting points to be noted in Fig. 5 are: the predicted displacement peaks shortly after the

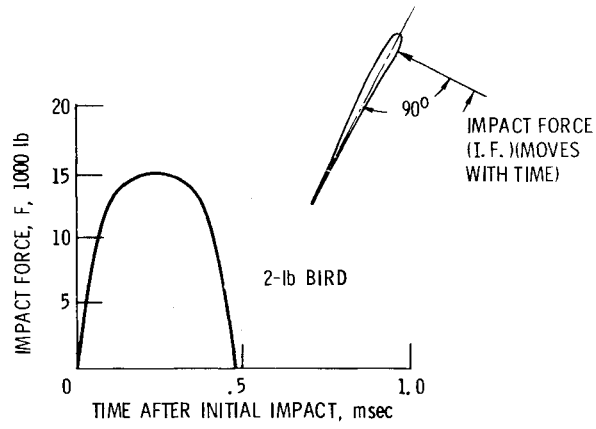

Fig. 4 Estimated impact force on hybrid composite fan blade (80% span, 2 lb bird, takeoff power).

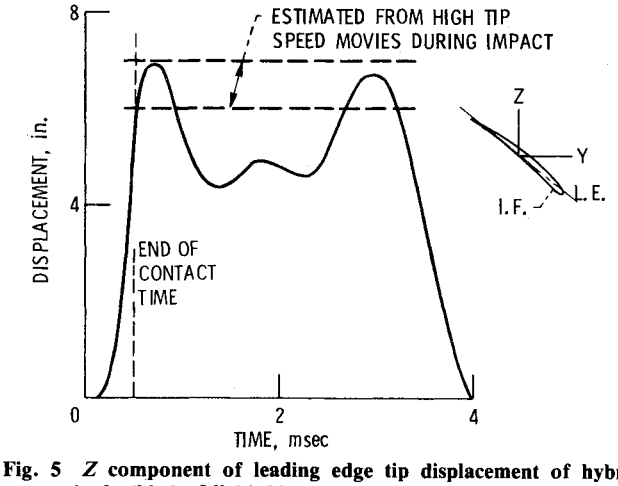

Fig. 5 *Z* component of leading edge tip displacement of hybrid composite fan blade, 2 lb bird impact.

impact time, the predicted displacement remains between about 4 and 7 in. for approximately 3 ms which corresponds to about 6 times the contact time, and the predicted displacement reaches the magnitude range which was estimated from high speed movies taken during impact.

Bending stresses on the suction surface at a point near the impact area are plotted vs time (assuming linear behavior and no fracture) in Fig. 6. The corresponding estimated strengths are also shown in the figure as straight lines parallel to the time axis. The most significant point to note in this figure is that the composite bending stresses reach their corresponding estimated strengths between about one-fourth and two-thirds of the contact time. This means that the impact conditions considered for this analysis will cause substantial local damage, and probably fracture, at very early times of the impact event. One logical conclusion is that the hybrid composite blade considered will not survive locally the imposed impact conditions. This conclusion is consistent with the local damage results.[1]

If it is assumed that no local fracture occurs at all, then it can be seen in Fig. 6 that: 1) the chordwise stress peaks at about 310 ksi at the end of the contact time, 2) the spanwise stress peaks at about −110 ksi about 0.8 times the contact time, and 3) the inplane shear peaks at about −153 ksi at about 1.5 times the contact time. Needless to say, both the chordwise and the inplane shear peak stresses are very high and will cause damage in any material. If no local failure occurs, the stresses at the base of the airfoil (grids 109-115, Fig. 2) peak at about 2.0 times the contact time. In this region

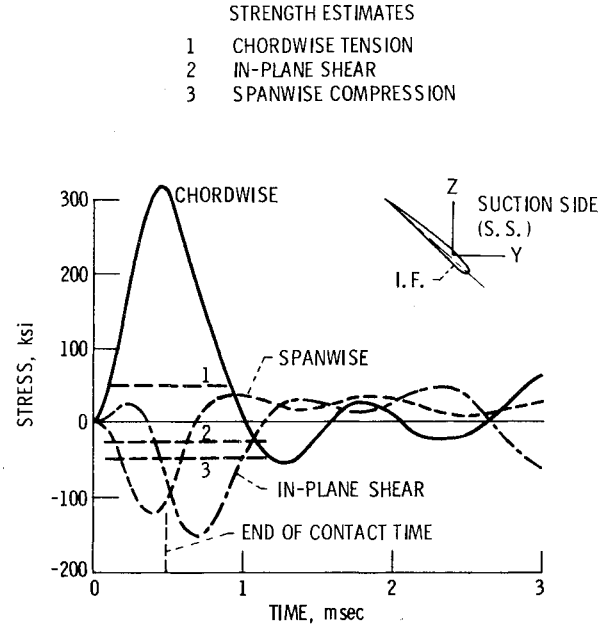

Fig. 6 Composite bending stresses near impact point (suction side) of hybrid composite fan blade, 2 lb bird impact.

also the chordwise and inplane shear composite stresses are higher than the corresponding estimated strengths. At midchord for example, the peak chordwise stress is 90 ksi (compared to an estimated strength of 45 ksi) and the inplane shear is 44 ksi (compared to 25 ksi). The spanwise composite stress, on the other hand, is about 80 ksi (compared to 90 ksi). A logical conclusion from the previous discussion is that the imposed impact conditions would probably cause root failures in the hybrid composite blade considered if no local failure occurs at the impact region.

It is noted that once damage has occurred, then some kind of nonlinear analysis is needed in order to determine the subsequent dynamic response of the hybrid composite blade.

Summary of Results

The significant results of an investigation to perform an analysis of a hybrid composite blade subjected to high velocity impact are as follows:

1) A computerized analysis capability was used which couples NASTRAN with a composite mechanics code to predict the dynamic response of hybrid composite blades prior to initial damage.

2) Predicted results from this capability for vibration frequencies and stresses were in good agreement with measured data.

3) Predicted tip displacements due to impact are in agreement with those magnitudes observed in high speed movies of the impact event.

4) The predicted stresses reach magnitudes comparable to the corresponding composite strength at early times during the impact event.

5) The impact conditions considered in this investigation are sufficiently severe to cause both local damage at early impact times (fraction of the contact time) as well as root failure at later times.

References

[1] Oler, T. L., "Fiber Composite Fan Blade Impact Improvement Program, Final Report," work performed under contract by General Electric Co., NASA CR-135078, 1976.

[2] McCormic, C.W., "NASTRAN User's Manual (Level 15)," NASA SP 222(01), 1972.
[3] Chamis, C.C., "Computer Code for the Analysis of Multilayered Fiber Composites—User's Manual," NASA TN D 7013, 1971. Compressor Blades: Vibration and Strength Analysis," NASA TM X-71589, 1974.
[4] Chamis, C.C. and Lynch, J.E., "High-Tip-Speed Fiber Composite Compressor Blades: Vibration and Strength Analysis," NASA TM X-71623, 1975.
[5] Chamis, C. C. and Minich, M. D., "Structural Response of Fiber Composite Fan Blades," ASME Publication 75-GT-78, 1975; also NASA TM X-71623, 1975.
[6] Chamis, C. C., "Vibration Characteristics of Composite Fan Blades and Comparison with Measured Data," *Journal of Aircraft*, Vol. 14, July 1977, pp. 644-647; also NASA TM X-71893, 1976.

Effect of Asymmetric Drag Polar Characteristics on Minimum Trimmed Drag

Gottfried Sachs*
Hochschule der Bundeswehr München, Neubiberg, Germany

Nomenclature

AR	= aspect ratio
b, b_t	= wing span, tail span
C_D	= drag coefficient
C_L	= lift coefficient
C_m	= pitching moment coefficient
e	= Oswald's efficiency factor, $k = 1/(\pi e AR)$
e_{rel}	$= e_{wb}/e_t$
h, h_{opt}	= center of gravity (c.g.) position in chord length, optimum c.g. position
h_t, h_{wb}	= aerodynamic center in chord length for tail, wing-body combination
k	= lift-dependent drag, $C_D = C_{D_0} + k(C_L - C_{L_0})^2$
S, S_t	= wing area, tail area
$\bar{\epsilon}_\infty$	= downwash angle at downstream infinity
$\epsilon_0^*, \epsilon_L^*$	= downwash factors

Subscripts

t	= tail
wb	= wing-body combination

IN recent papers,[1-10] the problem of reducing trimmed drag of the airplane has been investigated and it has been shown how lift must be distributed between the wing and tail in order to obtain the minimum of trimmed drag. The drag polars used in analytical relations for minimum trimmed drag are of the following type

$$C_D = C_{D_0} + kC_L^2 \tag{1}$$

As illustrated in the left part of Fig. 1, this expression can be characterized as a form which is symmetric with respect to the C_D axis. In many cases, however, the actual drag polars significantly deviate from this form and are as shown in the right part of Fig. 2. This type can be qualified as a drag polar with asymmetric characteristics. It may be analytically expressed as

$$C_D = C_{D_0} + k(C_L - C_{L_0})^2 \tag{2}$$

As can be seen, the quantity C_{L_0} provides a measure for the kind of asymmetric characteristics which are to be considered in the following.

There may be different reasons for the asymmetry addressed. One reason is camber of wing profile or, equivalently, flap deflection. An example is shown in part A of Fig. 2. From this it follows that drag polar asymmetry can be quite significant, being increased the more camber and/or flap angle is introduced. This effect may be of particular interest in regard to more recent designs utilizing new techniques such as "automatic maneuver flaps" or "variable wing camber." Here, leading- and trailing-edge flaps or variable camber are used to reduce drag at high lift in order to improve the maneuver performance of the aircraft. This is achieved by automatically operating the high-lift devices such that the highest lift drag ratio possible at each lift coefficient is obtained for the wing. However, wing drag polar asymmetry introduced by flap deflection or variable wing camber may have quite a significant effect on overall trimmed drag and may even influence the optimum tail contribution to minimum trimmed drag to a considerable extent. Moreover, the c.g. position related to minimum trimmed drag is also affected since, as will be shown, it is sensitive to the drag asymmetry addressed.

Another reason for asymmetric drag polar characteristics is wing twist. This is illustrated in part B of Fig. 2, which shows

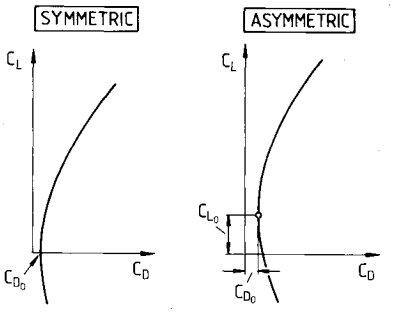

Fig. 1 Symmetric and asymmetric drag polar.

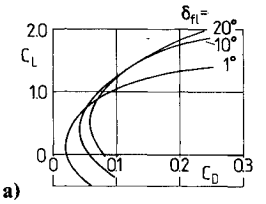

a)

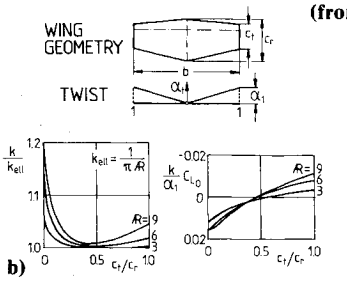

b)

Fig. 2 Drag polar asymmetry: a) Effect of flap deflection δ_{fl} (from Ref. 11); b) Effect of twist (from Ref. 12).

Received Feb. 15, 1980.

Index categories: Performance; Aerodynamics; Configuration Design.

*Professor of Flight Mechanics. Member AIAA.